

Research Paper

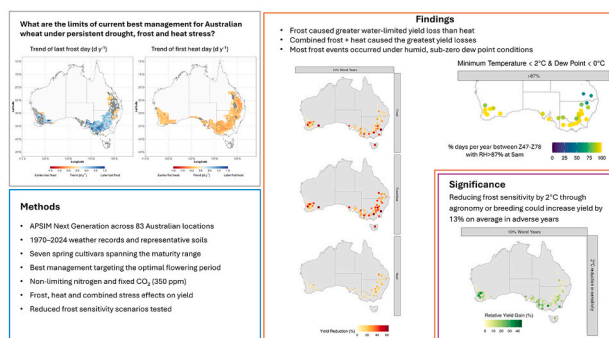
Shifting prospects for wheat production: Long-term simulation-based insights under best management in Australia

M. Fernanda Dreccer^{a,*}, Bangyou Zheng^a, Pengcheng Hu^b, Loretta Clancy^a, William Short^c, Karen Tanino^c^a CSIRO Agriculture and Food, St Lucia, QLD, Australia^b CSIRO Agriculture and Food, Black Mountain, ACT, Australia^c Department of Plant Sciences, College of Agriculture and Bioresources, University of Saskatchewan, Saskatoon S7N 2V3, Canada

HIGHLIGHTS

- Long-term wheat simulations under best management in Australia reveal thermal stress.
- Yield declines persist despite alignment with optimal flowering period.
- Frost events exceeded heat events between booting and early grain filling.
- Frost events were consistent with dew condensation preceding freezing.
- Reducing frost sensitivity by 1–2 °C could boost yield by up to 13% in adverse years.

GRAPHICAL ABSTRACT



ARTICLE INFO

Editor: T SCHUT

Keywords:

Wheat
Temperature
Water-limited yield
Yield potential
Heat
Frost
Optimal flowering period

ABSTRACT

CONTEXT: Wheat production in Australia remains vulnerable to climate variability, particularly to drought, late spring frost, and early heat during reproductive stages. Understanding how temperature extremes affect yield trends under best practice management is critical for improving production under changing conditions.

OBJECTIVE: To assess long-term changes in frost and heat exposure, quantify their impact on wheat yield trends, and evaluate the effectiveness of current adaptation strategies, including reduced frost sensitivity.

METHODS: APSIM Next Generation simulations were conducted across 83 locations using long-term weather records (1970–2024) and genotypic variation in phenology and the optimal flowering period (OFP) methodology. Simulations were run under best management conditions, with non-limiting nitrogen supply and CO₂ fixed at 350 ppm to isolate temperature-driven effects. Analyses focused on shifts in the timing of last frost and first heat, trends in yield potential and water-limited yield, characteristics of frost events and scenario analysis modifying frost damage thresholds in an empirical function.

RESULTS AND CONCLUSIONS

Shifts towards later frost and earlier first heat increased the likelihood of thermal stress during the OFP. Yield potential and water-limited yield declined over time across regions, even when flowering occurred within the OFP, indicating that exposure to interacting climatic stresses persists despite phenological optimisation. Frost

* Corresponding author.

E-mail address: Fernanda.dreccer@csiro.au (M.F. Dreccer).<https://doi.org/10.1016/j.agsy.2026.104837>

Received 8 January 2026; Received in revised form 18 May 2026; Accepted 28 May 2026

Available online 7 June 2026

0308-521X/© 2026 The Authors. Published by Elsevier Ltd. This is an open access article under the CC BY-NC license (<http://creativecommons.org/licenses/by-nc/4.0/>).

events were more frequent than heat events between booting and early grain filling, with up to 9.5 frost days recorded in the worst 10% of seasons. Most frost events occurred under high humidity and dew point temperatures below 0 °C, consistent with dew condensation preceding freezing. Scenario analyses showed that empirically reducing frost sensitivity by 1–2 °C increased yields by 7.3% and 13.4% respectively in adverse seasons, with minimal impact on OFP timing. This suggests yield gains under best management arise primarily from reduced crop sensitivity, with additional benefit from improved alignment between critical reproductive stages and reduced exposure to drought and heat.

SIGNIFICANCE: Model simulations demonstrate that climate variability is increasing spring frost risk in Australian wheat farming systems, exposing the limits of adaptation strategies based solely on phenological optimisation and highlight opportunities to enhance wheat resilience through agronomic innovation, targeted breeding, and improved modelling, supported by better understanding of frost type, canopy-level microclimate, and ice nucleation processes. Together, they show that improving wheat system resilience will depend not only on when crops flower, but on reducing how vulnerable they are to frost during critical reproductive stages.

1. Introduction

Numerous global and regional impact modelling studies have demonstrated that drought and high temperature, both historically and in future climate scenarios, are strongly associated with declines in ecosystem performance and crop yields. These studies utilise a range of methodologies. For example, using gridded climate data, Lobell and Field (2007) found that growing season temperature and precipitation explained ca. 30% of year-to-year variation in a range of crops. Lesk et al. (2016), using a statistical model, concluded that between 1964 and 2007, extreme drought and heat events led to a 9–10% drop in global cereal production. A crop multi-model ensemble study by Asseng et al. (2015), projected wheat yield losses of 6% °C⁻¹ temperature increase across diverse locations. In Eastern Africa, Adhikari et al. (2015) identified wheat as the most vulnerable crop under future climate scenarios, with current yields projected to decline by 48% by 2050. Using a more empirical method, the yield gap methodology, Gerber et al. (2024) warn about yield stagnation in wheat.

Beyond general temperature effects, experiments have demonstrated that specific thermal dynamics, such as night time warming, an expression of temperature asymmetric change, can significantly impact crop performance. García et al. (2015) reported a 7% yield loss per °C increase in nighttime temperature during critical stages of wheat and barley development. Spring frost, though often overlooked in climate impact assessments and more difficult to manipulate experimentally, also poses a significant threat to crop production and natural vegetation. Zohner et al. (2020), in a global study of temperate and boreal trees, found that late spring frost risk decreased in North America but increased in Europe and Asia between 1959 and 2017. In Australia, where spring frost coincides with the sensitive reproductive period of wheat, Zheng et al. (2015) documented an increase in frost events, a delay of the last frost and a significant increase in frost impact on wheat yields in certain areas of the cropping belt between 1957 and 2013. Crimp et al. (2016) further reported a lengthening of the frost season in southern Australia between 1986 and 2014, due to delayed last frost. More recent studies, also alert to the damage caused by spring frost in winter wheat in South Korea (Kim et al., 2025) and China (Zhao et al., 2024).

These insights highlight the complexity of thermal stress and its ongoing impact on crop productivity. While farmers, agronomists, and plant breeders have implemented a range of adaptation strategies, variation in yield and risk remains. The critical question is: what challenges persist in managing water stress and extreme temperatures once these adaptations are in place? This study addresses that question in the context of Australian wheat production, with a particular focus on spring frost during the reproductive stage, a persistent and multifaceted stressor that continues to affect yield stability despite adaptation efforts.

Australia's climate has warmed by 1.51 ± 0.23 °C since national records began in 1910. Since the 1970s, these changes have coincided

with a decline in cropping season rainfall (April–October), 16% in the southwest and 9% in the southeast, with the southwest experiencing a 20% reduction in May–July rainfall, traditionally key planting rainfall opportunities (State of the Climate 2024: Bureau of Meteorology). While gradual warming within the optimal temperature range primarily shifts phenological patterns, extreme events cause irreversible damage (Sadras and Dreccer, 2015). One consequence of the former is the acceleration of development in traditional cultivars sown in autumn in the Southern hemisphere, increasing the risk of cold damage during spring, coinciding with reproductive stages (Zheng et al., 2012).

Within the constraints of restricted water availability, farmers try to minimise yield loss by choosing planting dates and cultivar combinations that lead to flowering within a window with minimal impact of both water stress and extreme temperature in the long-term, known as the Optimal Flowering Window (OFP) (Flohr et al., 2017; Lilley et al., 2019). Adaptation strategies such as cultivar selection and sowing date adjustment can significantly buffer yield losses under elevated temperatures (Challinor et al., 2014). However, Hochman et al. (2017) reported stagnation in simulated water-limited wheat yields in Australia between 1990 and 2015, attributing this to warming-induced acceleration of crop development. Their study did not account for extreme temperature impacts but noted that on-farm yield losses were partially offset by technological advances. For instance, wheat breeders have contributed to a positive GxExM adaptation in the Australian farming system by releasing cultivars with stronger vernalisation requirements, enabling earlier sowing under autumn rainfall, avoiding now uncertain traditional planting rainfall opportunities and stabilising flowering time (Hunt et al., 2019; Zheng et al., 2016).

This study investigates the challenges of wheat production in Australia under best management practices, with a particular focus on frost during the reproductive stage. Using long-term weather records (1970–2024), genotypic variation in phenology across representative locations, and the APSIM Next Generation (NG) simulation model, the analysis addresses five key questions regarding climate-crop interactions. These include shifts in the timing of last frost and first heat days over time and their influence on the optimal flowering period (OFP); temporal variation in yield potential and water-limited yield across cultivars of differing maturity types when sown to flower within the OFP; and the extent to which frost and heat stress, individually and in combination, constrain water-limited yield under best-practice agronomy. The study also quantifies the frequency and meteorological conditions associated with damaging frost events during the sensitive reproductive phase and evaluates the potential yield benefits of reducing crop sensitivity to frost through genetic or agronomic interventions, particularly in years with extreme climatic conditions.

By addressing these issues, the study aims to clarify the limits of current adaptation strategies and identify opportunities to enhance resilience in wheat production under increasing climate variability.

2. Methods

2.1. Crop model, weather, soils and cultivars

Wheat phenology, growth, yield, water balance, and responses to frost and heat stress were simulated using the APSIM NG (version 2025.05.7755.0) (Holzworth et al., 2018) in 83 locations around the cropping belt, 77 reported by Lilley et al. (2019) and 6 by Chenu et al. (2013) (Supplementary Fig. 1, Supplementary Table 1). Yield was simulated as yield potential (genetics, radiation and temperature limited) and water limited yield. The APSIM NG model has been extensively validated for wheat across phenology, leaf area index, biomass and yield for a wide range of genotypes, environments and management (e.g. yield in Supplementary Fig. 2).

Weather data (1950–2024) were obtained from patched point meteorological weather stations (Jeffrey et al., 2001). Screen temperature (2 m height) was used, noting that temperatures at canopy height during frost events are typically 2–3 °C lower (Frederiks et al., 2012; Marcellos and Single, 1975). Soil profiles were sourced from Lilley et al. (2019) and Chenu et al. (2013), as stored in the APSOIL database (Dalglish et al., 2012). Simulations began in 1950, with analyses restricted to 1970 onwards to avoid residual effects from initial water and nitrogen inputs. Simulations assumed best management, with no nitrogen limitation, daily sowing between 15 April and 15 July, no annual soil water reset, and a small irrigation (15 mm) to ensure establishment. CO₂ was fixed at 350 ppm (1990 levels) to ensure model stability and comparability across years, isolating temperature-driven risks under best management.

Seven spring cultivars spanning the maturity spectrum, from quick to very slow, as per the boundary categories defined by Celestina et al. (2023) were used in the simulations (Supplementary Table 2) (Wang et al., 2025). These included Emu Rock (Quick), Mace (Quick-Mid), LRPB Trojan (Mid), Strzelecki (Mid-Slow), Beaufort (Slow), EGA Eaglehawk (Slow-Very Slow), and Sunlamb (Very Slow).

Frost and heat damage in APSIM NG were applied as daily post-processing yield penalties based on screen minimum and maximum temperatures, during crop-specific sensitive periods (Supplementary Fig. 3). The empirical damage functions were grounded in understanding of reproductive-stage sensitivity, yield loss increasing with stress severity (Cheong et al., 2019; Dolferus et al., 2011; Dreccer et al., 2014; Jagadish, 2020). Parameters were derived from multisite field datasets using cross-validated global optimisation and independently evaluated, resulting in crop-specific temperature thresholds and response functions that improved out-of-sample yield predictions relative to the original APSIM model. Losses accumulated multiplicatively, with final yield scaled by remaining fractions after frost and heat penalties; implementation is accessible via the APSIM NG GUI and source code (Supplementary Table 5).

2.2. Optimal flowering period (OFP)

For each location, the OFP was defined as the range of flowering dates achieving at least 95% of the peak mean long-term yield, through a combination of sowing date and cultivar selection, following Lilley et al. (2019) and Hu et al. (2021) with modifications reflecting long-term simulations (1970–2024) and explicit inclusion of frost and heat impacts on yield. Daily simulated frost and heat limited yield potential and water-limited yield were analysed across flowering dates. For each sowing date, the yearly outputs were grouped, and the mean values of yield and flowering dates per cultivar were calculated. At each site, the OFP corresponds to any of the seven cultivars that achieved minimum 95% of the peak mean long-term yield. The mid-point (flowering date with highest long-term mean yield) and span of the OFP were calculated, and their temporal dynamics assessed using a 20-year moving window.

Statistical significance of the linear trends in mid-point and span was evaluated by a *t*-test ($\alpha = 0.1$) accounting for temporal auto correlation (Santer et al., 2000).

2.3. Frost and heat events

Temporal trends in last frost and first heat were analysed using daily SILO gridded climate data (Jeffrey et al., 2001) (0.05° × 0.05°, ~5 km resolution) for 1970–2024 following Zheng et al. (2015). Frost and heat were defined as $T_{min} \leq 0$ °C and $T_{max} \geq 34$ °C, respectively. The last frost day was defined as the 90th percentile of $T_{min} \leq 0$ °C, and the first heat day was defined as the 30th percentile of $T_{max} \geq 34$ °C. Temporal shifts in these dates assessed over 1970–2024. Across most of mainland Australia, the 90th percentile of last frost occurred between July and October, later in Tasmania. Trends were tested using a *t*-test ($\alpha = 0.1$) accounting for temporal autocorrelation (Santer et al., 2000).

2.4. Dew point temperatures analysis

To support dew point temperature analysis during early morning hours, when frost risk is high, relative humidity measurements taken at dawn (5 am) from patched point meteorological stations (2 m height; Jeffrey et al., 2001) were used. These measurements have been consistently available only since 2015. Consistent data availability from 2015 onwards, combined with a $\geq 90\%$ coverage criterion, resulted in 29 reliable stations across the cropping belt (Supplementary Fig. 4). Weather data were filtered to the frost sensitive period defined in the yield reduction function (Supplementary Fig. 2), i.e. from flag leaf sheath opening (Z47) to late milk (Z77) for 2015–2024. Dew point temperature was calculated as:

$$\gamma = \frac{aT}{b + T} + \ln\left(\frac{RH}{100}\right)$$

$$T_{dew} = \frac{b\gamma}{a - \gamma}$$

where T is minimum air temperature (°C), RH is the relative humidity (%), $a = 17.62$ and $b = 243.12$; γ varies with T and RH (Alduchov and Eskridge, 1996).

Leaf wetness was estimated following (Wichink Kruit et al., 2004), as validated by Gama et al. (2022) and Sentelhas et al. (2008). Leaves were considered wet when $RH \geq 87\%$; for RH between 70 and 87%, wetness depended on changes in RH (>3% increase in 30 min for wetting; > 2% decrease for drying); leaves were assumed dry when $RH < 70\%$.

2.5. Impact of decreasing frost sensitivity

Different levels of frost sensitivity were simulated by modifying the empirically derived daily yield reduction function, lowering the temperature at which damage can occur. The default function (damage increasing below 1 °C) was compared with scenarios starting at 0, –1 and –2 °C, while keeping the maximum damage threshold constant at –4 °C (Supplementary Fig. 5). Simulations were re-analysed to determine (i) shifts in the OFP, (ii) relative yield gain and (iii) the number of events during sensitive stages. Yield (Y) gain (G_t) was calculated as:

$$G_t = \frac{Y_{Dt} - Y_D}{Y_D} \times 100$$

Where Y_D and Y_{Dt} are water limited yield without frost stress and water limited yield with frost stress as illustrated in Supplementary Fig. 5 for the default and the three reduced frost sensitivity scenarios ($D_{-1} = 0$ °C, $D_{-2} = -1$ °C and $D_{-3} = -2$ °C) with respect to the default function ($D = 1$ °C) at a representative location.

3. Results

3.1. Have dates of last frost and first heat changed?

The first heat day is occurring significantly earlier, by 0.5 d y⁻¹ or more, while the last frost day is occurring later, by 1 d y⁻¹ or more where trends are significant, particularly in the southeast (Fig. 1(a) and 1(b)). In locations with significant trends, the 90th percentile for last frost day (T_{min} ≤ 0 °C) occurred between mid-August and mid-October, indicating that in 9 out of 10 years, frost events occur on or before these dates (Fig. 1(c)). Conversely, the 30th percentile for first heat day (T_{max} ≥ 34 °C after July 1st) occurred from late September onwards, marking the earliest onset of heat events in 3 out of 10 years (Fig. 1(d)). The narrowing interval between these percentile thresholds suggests an

increased probability of crops being exposed to either late frost and/or early heat during sensitive phenological stages, thereby increasing the risk of thermal stress and yield loss.

3.2. Have yield potential and water limited yield changed between 1970 and 2024?

In this study, both the yield potential and water limited potential were simulated under best practice agronomy and met the criteria defined for the optimal flowering period (OFF), i.e. with each variety flowering at a date achieving at least 95% of the peak mean long-term yield. Analyses were conducted across different maturity groups to examine long-term yield outcomes using phenology as an integrative framework through which warming, frost and heat timing, water

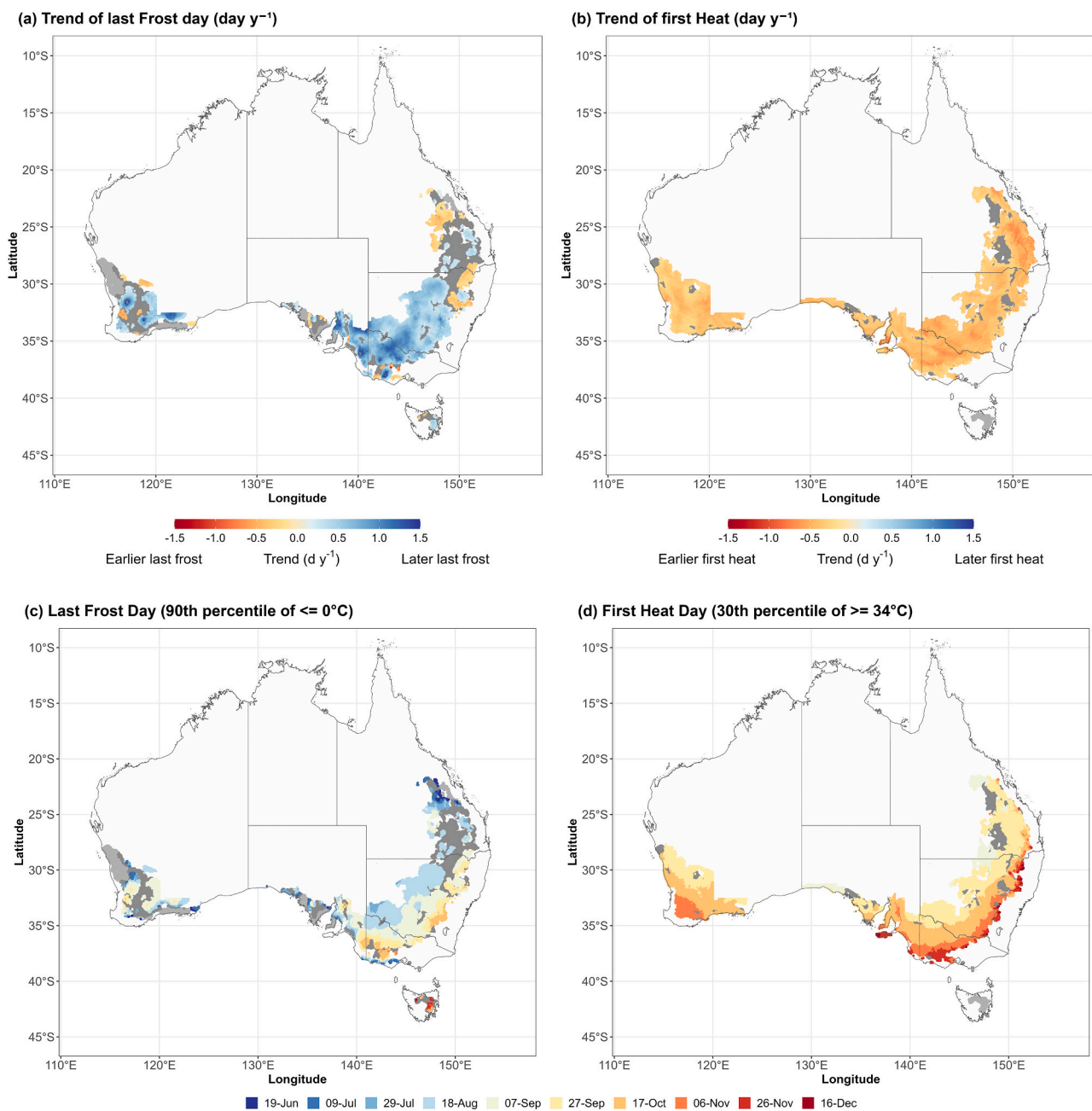


Fig. 1. Temporal trends in last frost (a) and first heat day (b) between 1970 and 2024. Last frost day is T_{min} ≤ 0 °C and first heat day is T_{max} ≥ 34 °C after July 1st. Date of last frost day (90th percentile) (c) and date of first heat date (30th percentile) (d). Coloured cells where the trend was significantly different from 0 (*P* < 0.1). Light grey cells indicate areas with no frost or heat; dark grey cells indicate no change.

limitation, and changes in OFP properties jointly influence productivity.

Yield potential, constrained only by temperature, radiation and cultivar genetics declined across the cropping belt and among different maturity groups between 1970 and 2024. On average, yield potential declined by $15 \text{ kg ha}^{-1} \text{ yr}^{-1}$ for quick-maturing varieties and $19 \text{ kg ha}^{-1} \text{ yr}^{-1}$ for slow-maturing varieties across all sites. When considering only sites with significant trends (approximately 28 out of 83), the decline

was around $11 \text{ kg ha}^{-1} \text{ yr}^{-1}$ for quick and mid-maturity types, and $17 \text{ kg ha}^{-1} \text{ yr}^{-1}$ for slow types (Fig. 2, Supplementary Table 3). While some sites exhibited significant decline in yield potential for only one or two maturity groups, others showed decline across all maturity groups. Sites such as Birchchip in Victoria, Tarlee in South Australia and Parkes in New South Wales are among those that showed a decline in yield potential across the different maturity groups.



Fig. 2. Temporal trends in yield potential (a) and water limited yield (b) in 83 sites between 1970 and 2024 for a quick (Emu Rock), a quick-mid (Mace) and a slow (Strzelecki) maturing variety. Grey circles indicate sites with no significant trend over time ($P \geq 0.1$), based on a *t*-test that accounts for temporal autocorrelation (Santer et al., 2000). Coloured circles represent sites with significant trends, indicating the direction and magnitude of change, while size indicates magnitude ($\text{kg ha}^{-1} \text{ year}^{-1}$).

Simulated water limited yield, constrained by temperature, water availability, radiation and cultivar genetics, also showed a declining trend. Across all sites, average declines were approximately $17 \text{ kg ha}^{-1} \text{ yr}^{-1}$ for quick maturing and quick-mid maturing varieties, and $25 \text{ kg ha}^{-1} \text{ yr}^{-1}$ for slow maturing varieties. Among sites with significant declines, water-limited yield potentials were 18, 15 and $22.5 \text{ kg ha}^{-1} \text{ yr}^{-1}$ for the quick, quick-mid, and slow varieties respectively, based on 54, 40, and 29 out of 83 sites (Fig. 2, Supplementary Table 4).

In comparison, quick varieties experienced smaller significant reductions in water limited yield over time, in more locations, compared to slow maturing varieties. The greatest losses were more frequently observed in the southeast region of the cropping belt.

3.3. Trends in the optimal flowering period (OFP) under water limited conditions

The optimal flowering period under water limited conditions was estimated for each site, for the cultivar x sowing date combination maximising yield in the long-term. Significant variation in the mid-point was observed in 31 out of 83 locations, trending to later dates, and in 41 out of 83 sites for the span, contracting by up to 1 d y^{-1} (Fig. 3).

3.4. What is the impact of frost and heat individually and in combination on water limited yield under best practice?

To investigate the impact of frost and heat, individually or in combination, on simulated water-limited yields, scenarios including frost damage, heat stress, or both were compared to a baseline simulation that accounted for water limitation only.

The reduction to the water limited yield due to frost was generally greater than that due to heat alone (Fig. 4). In the 10% of years with highest yield losses, frost-related water limited yield reduction ranged from no change to more than 50% depending on location, with a median of 16%, while heat-related reductions ranged from no change to ca. 30%, with a median of 6%. The combined effect of frost and heat caused greater reductions in water-limited yield than either stress alone (Fig. 4 and Supplementary Table 5). This pattern was consistent across locations, particularly in years representing the worst 1 in 4 (25% worst) and 1 in 10 (10% worst) seasons for yield losses. These comparisons reflect relative impacts under the applied empirical framework; they do not imply complete biological separation of frost-only and heat-only effects.

3.5. Frost characteristics: number of events

In wheat crops sown to maximise yield by flowering in the OFP, the number of frost events while the crop was sensitive according to the model function for yield reduction due to frost, i.e. from Zadoks 47 to 78

(Supplementary Fig. 3), was greater than for heat (Fig. 5). During the worst 10% of years, one location experienced up to 9.5 frost events in this period. Across 83 sites, the average number of frost events was approximately 4, and only 7 sites did not experience any frost (Fig. 5).

3.6. Frost characteristics: relative humidity and dew point temperature

Dew point temperature is a critical indicator of frost risk, as it determines whether moisture condenses as dew or freezes on plant surfaces or whether the plant surface is devoid of moisture during the freezing event, directly influencing the likelihood of crop damage.

Dew point was calculated using measurements taken at the standard weather station height of 2 m, where minimum temperature and relative humidity are recorded, during the crop's sensitive period according to the model function (Supplementary Fig. 3). Because the minimum temperature at canopy height (0.7–0.9 m) is typically $2\text{--}3 \text{ }^\circ\text{C}$ lower than at screen height (Marcellos and Single, 1975), a $2 \text{ }^\circ\text{C}$ offset was applied to approximate canopy conditions, assuming this corresponds to $\sim 0 \text{ }^\circ\text{C}$.

To better characterize conditions associated to freezing events, relative humidity was grouped into three categories: wet ($\geq 87\%$), transitioning (70–87%), and dry ($< 70\%$), linked to leaf wetness (see Materials and Methods). When minimum temperature fell below $2 \text{ }^\circ\text{C}$, the number of occurrences varied depending on dew point: 1919 events per year were recorded when dew point was $\geq 0 \text{ }^\circ\text{C}$, compared to 1241 when it was below $0 \text{ }^\circ\text{C}$ (Fig. 6). Events with dew point above $0 \text{ }^\circ\text{C}$ at screen height occurred only under $\text{RH} \geq 87\%$, conditions that favour liquid dew formation and may allow freezing at canopy level, although this cannot be confirmed. By contrast, when dew point dropped below $0 \text{ }^\circ\text{C}$ at screen height (2 m), conditions were more conducive to ice formation if canopy temperatures fell below freezing (Fig. 7). Among the 1241 records with minimum temperature below $2 \text{ }^\circ\text{C}$ and dew point below $0 \text{ }^\circ\text{C}$, 89% occurred under relative humidity $\geq 87\%$, while only 2.7% and 8.1% occurred under relative humidity $< 70\%$ and 70–87%, respectively. Within the high-humidity group, 98% of events corresponded to frost (minimum temperature $< 0 \text{ }^\circ\text{C}$ at screen height, and likely even lower at canopy height). A summary of relative humidity and temperature conditions per location in the lower-left quadrant of Fig. 7 is provided in Supplementary Fig. 6. As expected, relative humidity at the time of frost showed no correlation with minimum temperature (data not shown).

To assess the spatial patterns, daily weather records were filtered per location by minimum temperature below $2 \text{ }^\circ\text{C}$ and dew point temperature below or above $0 \text{ }^\circ\text{C}$ (Fig. 7). As expected, when dew point temperature was above $0 \text{ }^\circ\text{C}$, all events occurred under relative humidity above 87% (Fig. 7b). When dew point temperature was below $0 \text{ }^\circ\text{C}$, sites with relative humidity above 87% showed the highest frequency of frost-conductive events, expressed either as a count or as a percentage of

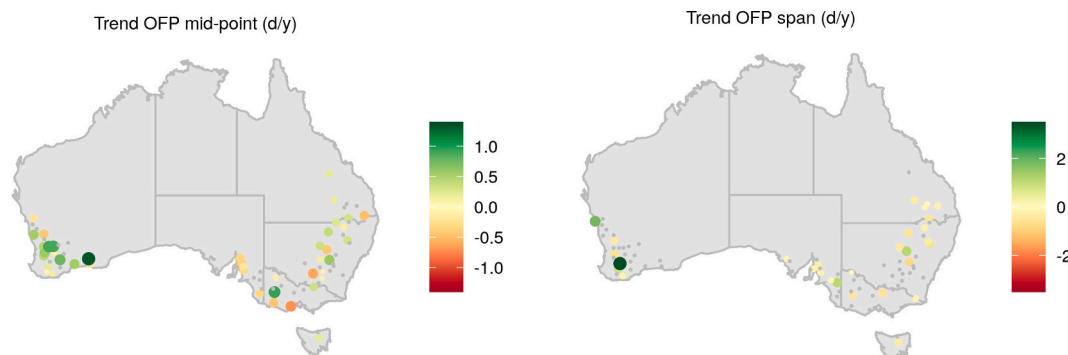


Fig. 3. Temporal trends in the optimal flowering period mid-point (left) and span (right). At each site, the OFP corresponds to the flowering dates at which cultivars achieved a minimum 95% of the peak mean long-term yield. Grey circles indicate sites with no significant trend over time ($P \geq 0.1$), based on a t-test that accounts for temporal autocorrelation (Santer et al., 2000). Coloured circles represent sites with significant trends, indicating the direction and magnitude of change, while size indicates magnitude (d y^{-1}).

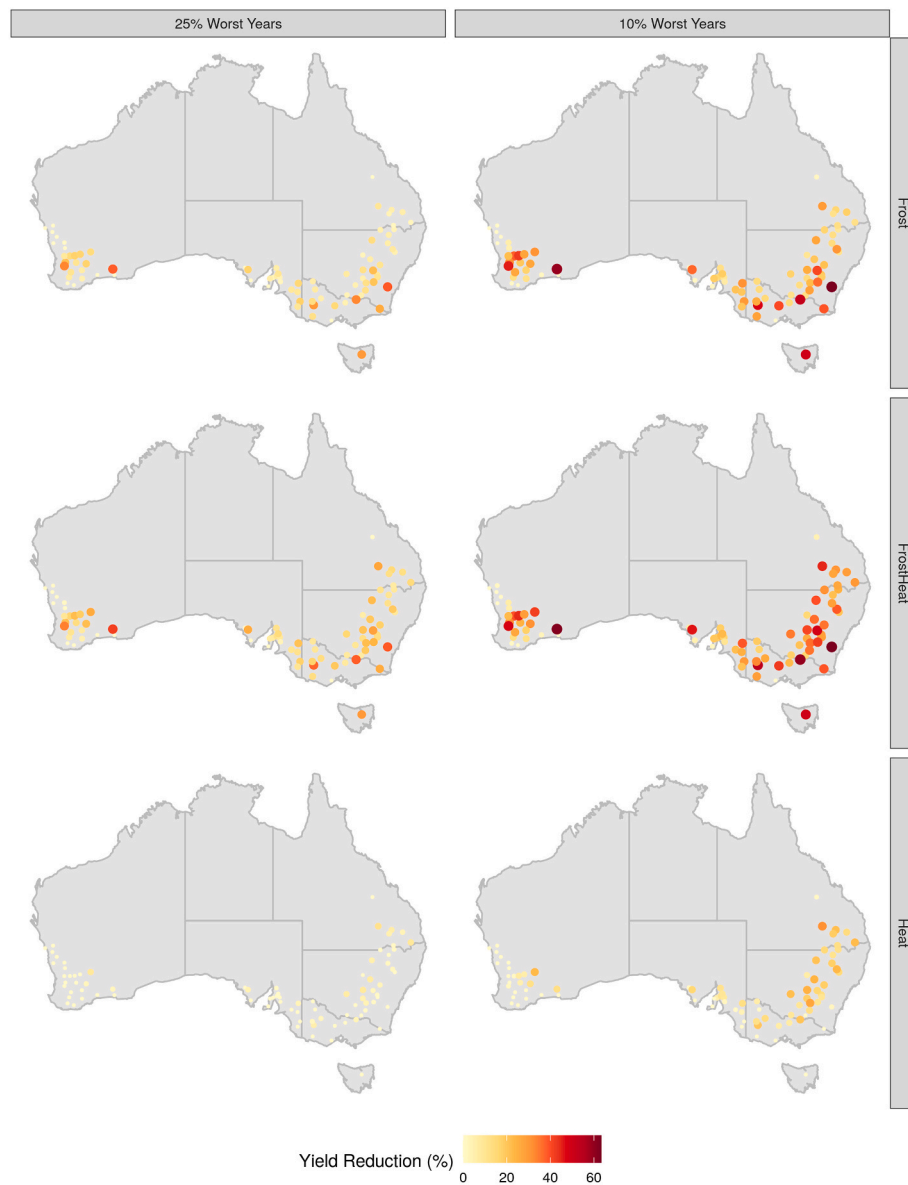


Fig. 4. Yield reduction due to the impact of frost (top row), heat (bottom row) and frost and heat (centre row) on water limited yield in the best performing cultivars per site. The left panel represents the 25% worst years, and the right panel represents 10% worst years for yield reduction between 1970 and 2024.

total events per location (Fig. 7a, Supplementary Fig. 6).

3.7. Impact of decreasing crop sensitivity to frost, particularly in worst-case scenario years

To investigate the potential gains based on management or genetic interventions, the threshold temperature (screen height) where frost damage starts in the APSIM NG damage function was reduced from 1 °C (D, default) to 0 °C (D₋₁), -1 °C (D₋₂) and -2 °C (D₋₃) (Supplementary Fig. 7). Therefore, the slope of sensitivity to frost damage increased from D₋₁ to D₋₃. The temperature at which maximum damage will occur was not changed, as it would be less likely to design an intervention that can prevent damage in this range.

Decreasing the sensitivity to minimum temperature shifted the midpoint of the OFP progressively more from D₋₁ to D₋₃. The OFP occurred on average 6 days earlier in D₋₁ (range: 1 to 27 days, 48 sites), 14 days earlier in D₋₂ (range: 1 to 29 days, 62 sites) and 16 days earlier in D₋₃ (range: 1 to 33 days, 65 sites) (Fig. 8). Interestingly, earlier OFP was not only observed for sites in the southeast but also in the west, with

even bigger shifts depending on the sensitivity scenario.

In the 10% worst years, yield gains would be on average 7.3% (range: 0.1 to 21.3%), 13.4% (range: 0.1 to 35.2%) and 17.2% (range: 0.1 to 45.2%) by D₋₁, D₋₂ and D₋₃ respectively in ca. 93% of locations, due to crops facing a lower number of events during the sensitive period compared to the default function (Fig. 9).

4. Discussion

4.1. Yield potential and water limited yield

Despite optimisation of flowering time and removal of nutrient constraints, long-term simulations revealed declining trends in both yield potential and water-limited yield across large parts of the Australian cropping belt. The direction of these declines is consistent with earlier modelling and observational studies, although their magnitude varies with cultivar choice, sowing rules, fertilisation strategies, representation of CO₂ responses, and the source and period of climate data (Hochman et al., 2017; Lawes et al., 2025). Extending the

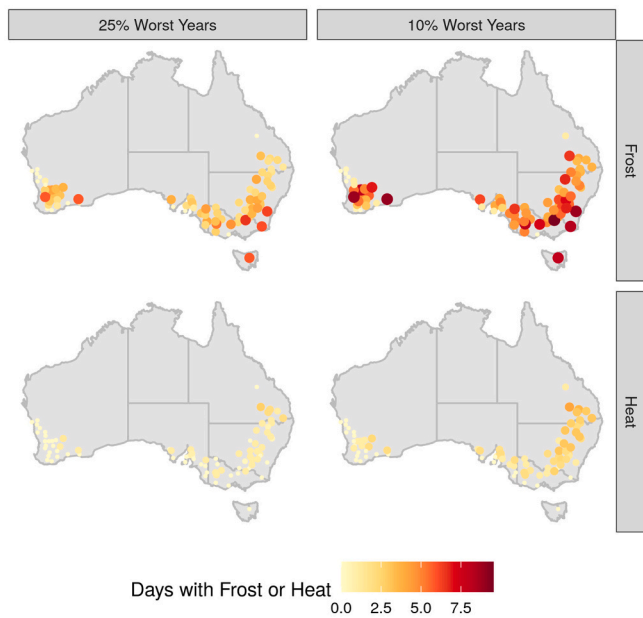


Fig. 5. Number of frost and heat days while the crop is sensitive according to the model function (Supplementary Fig. 2). The left panel represents the 25% worst years, and the right one represents the 10% worst years for yield reduction between 1970 and 2024.

analysis back to 1970 and applying the optimal flowering period (OFP) framework highlights the cumulative effect of climate variability under best-practice systems.

Within this context, cultivar phenology should not be interpreted as the primary causal driver of yield decline, but rather as an integrative axis through which interacting stresses operate. In Australian rainfed systems, phenology has been central to adaptation, underpinning management strategies such as modified vernalisation requirements combined with earlier and deeper sowing to stabilise flowering time under

shifting rainfall patterns (Flohre et al., 2017; Rebetzke et al., 2007; Hunt et al., 2019), as well as alternative approaches such as winter sowing of summer cereals to avoid heat and drought during reproduction (Rodriguez et al., 2024). While these strategies have been effective in buffering some climate impacts, the present results show that yield losses persist even when crops flower within the OFP. Taken together, these results suggest that, despite substantial breeding and agronomic innovation under increasing climatic variability, the benefits of phenology-based adaptation under best management have occurred against a backdrop of declining yield potential and water-limited yield, and are increasingly offset by persistent constraints and continued exposure to damaging reproductive-stage temperature stress, reinforced by delays in the timing of the last spring frost (Crimp et al., 2016; Li et al., 2015).

4.2. Impact of frost and heat stress on water limited yield

Even under best management, thermal extremes continued to constrain water-limited yield. Frost was the dominant stressor, causing larger losses than heat, especially in severe seasons, and the combined effect of frost and heat was greater than either stress alone. This likely reflects differences in timing and expression: frost is occurring more frequently and later in spring (Crimp et al., 2016; Li et al., 2015; Zheng et al., 2015), coinciding with critical stages such as pollen meiosis and anthesis (Cheong et al., 2019), when grain number is determined (Fischer, 1985). By contrast, heat more often acts through gradual warming that accelerates development and alters resource capture (García et al., 2015; Subedi et al., 2025). Severe heat events are more sporadic and tend to occur later in autumn-sown spring crops (Dreccer et al., 2018), mainly affecting grain filling and composition (Martínez-Subirà et al., 2021; Stone and Nicolas, 1995). Although early-season heat shock events can potentially cause significant damage (Jagadish, 2020), they remain relatively uncommon. The lower relative impact of heat observed here likely also reflects the role of the OFP framework, which reduces long-term exposure to severe water and heat stress by association, whereas frost is harder to avoid and can continue to reduce yield beyond flowering (Perry et al., 2017).

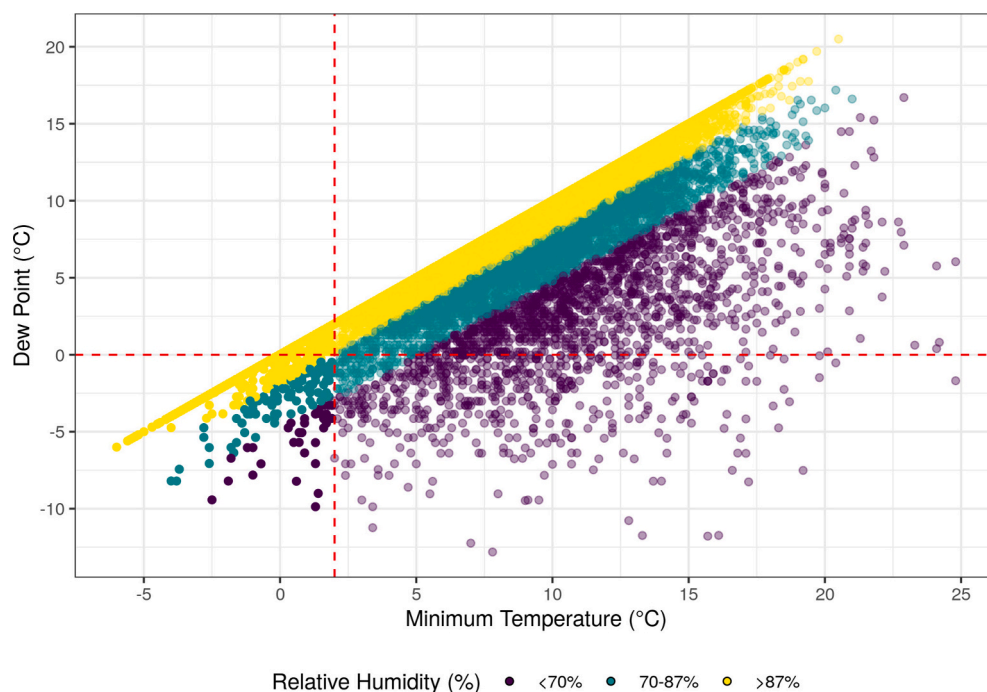


Fig. 6. Relationship between dew point temperature and minimum temperature at 29 sites, includes all events during the sensitive period between 2015 and 2024. Data have been separated into three relative humidity ranges, details in Methods. Note: Multiple data points overlap and may appear as a single point.

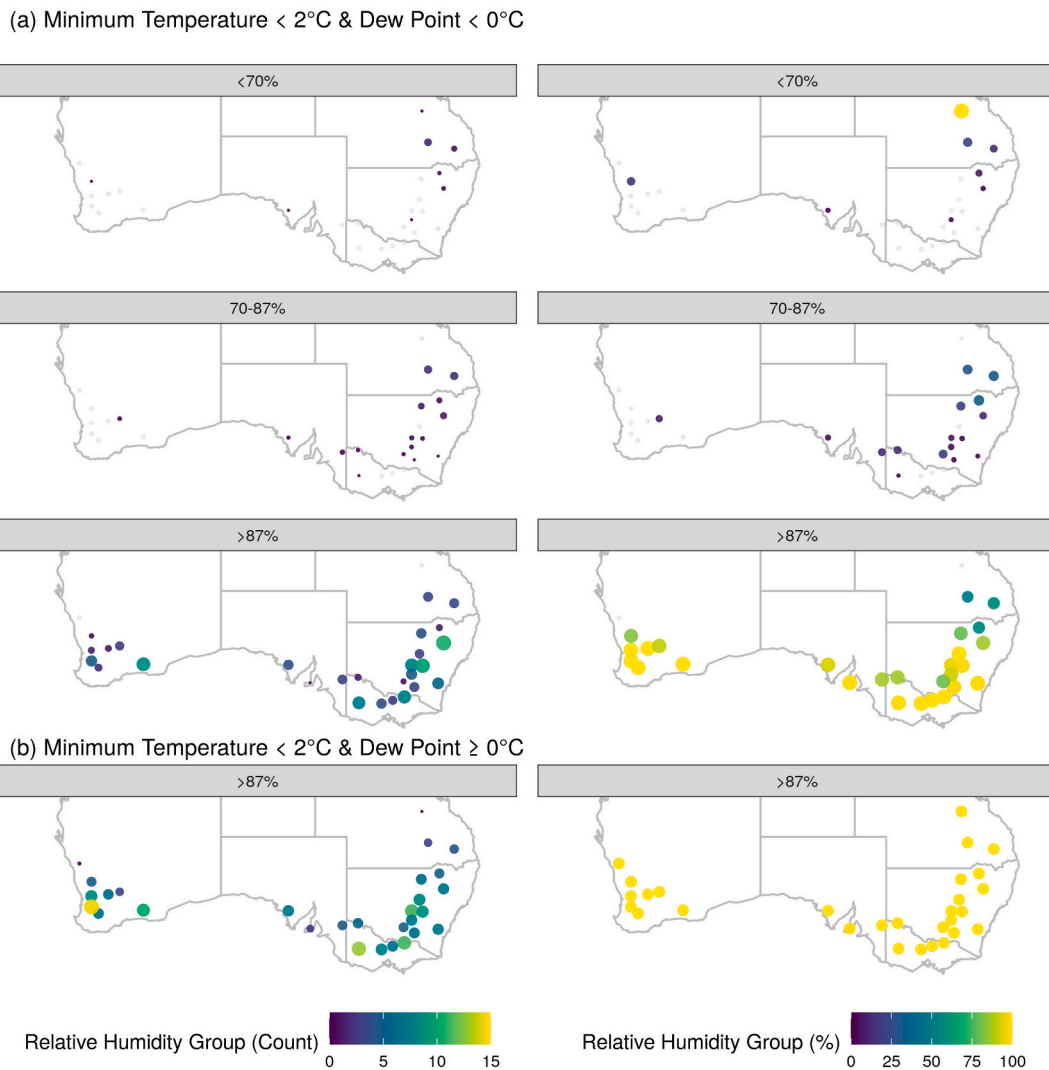


Fig. 7. Relative Humidity Group Count (left column) refers to the average number of days per year during the sensitive period in the model function (Zadoks 47–78) that met the specified temperature and dew point criteria. Relative Humidity Group (%) (right column) is the proportion of those days relative to the total number of days meeting the temperature condition across all humidity categories at each location. Panel (a) $T_{min} < 2^{\circ}\text{C}$ and dew point $< 0^{\circ}\text{C}$. Panel (b) $T_{min} < 2^{\circ}\text{C}$ and dew point $\geq 0^{\circ}\text{C}$. Event panels are grouped by relative humidity category (see Methods). Grey points are locations with no events registered for the category under study.

The relative importance of frost, heat, and their combined effects should, however, be interpreted in light of how thermal stress was represented in the model. The frost and heat damage functions used here provide a pragmatic large-scale representation of thermal stress through empirical daily yield penalties based on temperature thresholds and crop sensitivity. Although not mechanistic, they are grounded in current physiological understanding of sensitive stages and supported by field-based evidence, enabling consistent comparison of interacting stresses across environments and long-time series. These outcomes, however, remain contingent on interacting climatic conditions and stage-specific damage processes that are not explicitly resolved at the process level in the functions. By contrast, controlled-environment studies often rely on fixed conditions and synchronised phenology, which can limit the robustness and transferability of derived parameters to field conditions characterised by fluctuating temperatures, variable humidity, and phenological asynchrony (Xiao et al., 2022).

Future advances will require more mechanistic representations of frost and heat damage including processes governing grain number and grain filling (Barlow et al., 2015; Richetti et al., 2025), as well as resolving canopy energy balance and organ-level temperature dynamics (Webber et al., 2017). Capturing the effects of temperature variability, exposure duration, and damage processes will likely require higher

temporal resolution data alongside improved representation of spatial variability such as topography and wind exposure (Gobbett et al., 2021; Guo et al., 2024; Rapacz et al., 2022). In this context, the use of location-specific weather data in this study reduces uncertainty associated with spatial averaging and highlights the vulnerability of the southeast cropping belt to combined frost and heat stress under best-practice management.

4.3. Frost characteristics during the sensitive period: mechanisms and modelling implications

Frost damage in wheat depends not only on threshold temperature but also on the timing of sensitive stages and the atmospheric conditions governing freezing. Consistent with radiative frost, most damaging events during sensitive stages were associated with high humidity and low dew point conditions (0 to -5°C) frost (Román-Figueroa et al., 2021). Current modelling and monitoring approaches, however, rely largely on screen-height temperatures and lack canopy-level microclimate information, limiting their ability to capture the conditions under which damage actually occurs. Distinguishing between frost types, such as dew-associated freezing, depositional frost and internal freezing, therefore provides a more process-relevant basis for improving both risk

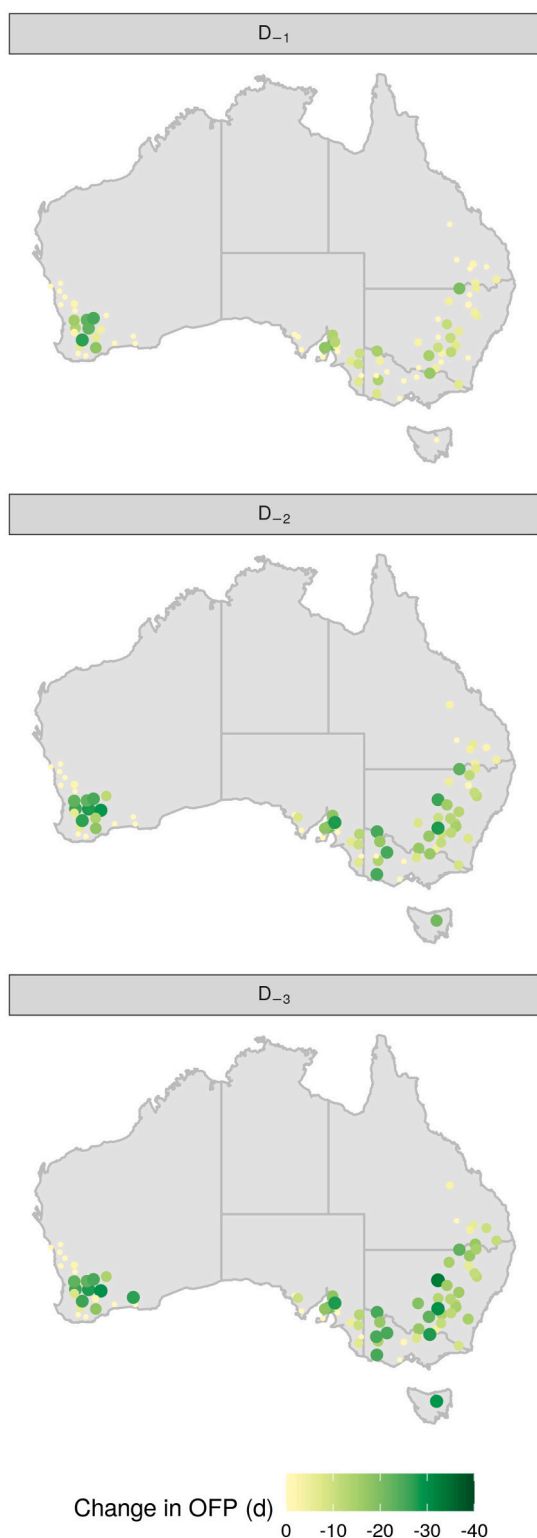


Fig. 8. Change in the OFP midpoint (days) towards earlier calendar days when the sensitivity to frost starts at 0 °C (D_{-1}), -1 °C (D_{-2}) and -2 °C (D_{-3}) with respect to the default function (1 °C). In the scale, 0 represents no change.

assessment and management.

Dew point temperature is central to the interpretation of frost risk because it determines whether moisture condenses or freezes on plant surfaces, directly influencing the likelihood of crop damage. Dew point was calculated using measurements taken at the standard weather-station height (2 m), noting that minimum temperature at canopy

height is typically 2–3 °C lower than at screen height (Marcellos and Single, 1975). This vertical temperature gradient implies that freezing conditions at the canopy can occur even when screen temperatures remain above nominal damage thresholds.

The pathway to frost damage depends strongly on the presence of water and ice nucleation processes. The occurrence of external nucleators, together with moisture such as dew during a frost event, reduces the ability of herbaceous plants to supercool (Wisniewski et al., 2009). Experimental evidence showed that dry wheat spikes can supercool down to -15 °C, whereas wet spikes (when water combined with ice nucleating bacteria) nucleate at considerably warmer temperatures (average at -4.5 °C) (Fuller et al., 2007). In the field, wheat at the post-spike emergence stage can be damaged at approximately -3.5 °C to -4.5 °C, and wax removal has been shown to increase susceptibility under high-humidity freezing, highlighting the importance of barriers to external nucleation (Single and Marcellos, 1974). Freezing may also initiate internally, with older tissues freezing before younger ones, which may retain greater supercooling capacity due to differences in composition and microbial load (Livingston et al., 2016, 2018, 2021). Taken together, these observations show that frost damage cannot be attributed to a single mechanism, reinforcing the need to resolve frost type and canopy conditions in field environments.

4.4. Impact of decreasing frost sensitivity

Within this environmental context, simulation results highlight crop sensitivity as a key lever for adaptation under conditions where phenological adjustment alone is insufficient. A modest reduction in frost sensitivity (1–2 °C) produced substantial yield gains in adverse seasons across most locations and was associated with a shift of the optimal flowering period (OFP) towards earlier dates. It is likely that yield gains arise primarily from reduced crop sensitivity, with additional benefit from improved alignment between critical reproductive stages and reduced exposure to drought and heat, thereby avoiding the trade-offs typically associated with strategies that delay flowering to escape frost.

From a breeding perspective, progress in reducing frost sensitivity has been limited. Gusta and Wisniewski (2013) attribute this to under-recognition of the diversity of dominant frost types and ice nucleation sources, difficulties in scaling traits from molecular or cellular levels to canopy level, and the limited transferability of controlled environment results to field conditions. Evidence in wheat indicates limited capacity for cold acclimation during reproductive stages, suggesting that plants may rely primarily on avoidance mechanisms rather than acquired tolerance (Fuller et al., 2007). Accordingly, avoidance traits such as waxiness, supercooling capacity, erect leaves and ice compartmentalisation can reduce ice formation and help avoid intracellular freezing, while tolerance traits such as membrane stability, osmotic adjustment, and accumulation of compatible solutes may mitigate damage once freezing occurs (Gusta and Wisniewski, 2013; Rahman et al., 2021; Wisniewski et al., 2009).

Agronomic strategies remain an essential part of the solution to managing frost risk. Landscape position, exposure, and soil properties influence frost occurrence and severity (Boer et al., 1993; Gobbett et al., 2021) and while phenology-based strategies can reduce risk, they do not eliminate it (Zheng et al., 2016). Management options such as soil modification by delving have shown promise by increasing soil and canopy temperatures but are costly, and effectiveness is limited to sandy topsoils (Rebbeck et al., 2007), while high residue loads in conservation systems may exacerbate frost damage by lowering soil temperatures (Flower et al., 2022). Varietal mixtures offer potential for buffering stress impacts through asynchronous responses (Fletcher et al., 2016; Stefan et al., 2024, 2025), though trait-level understanding of plasticity within a mixture under frost remains unexplored. In-season management options are currently limited but include growth regulators, grazing, and apical pruning to stagger flowering (Porker et al., 2022).

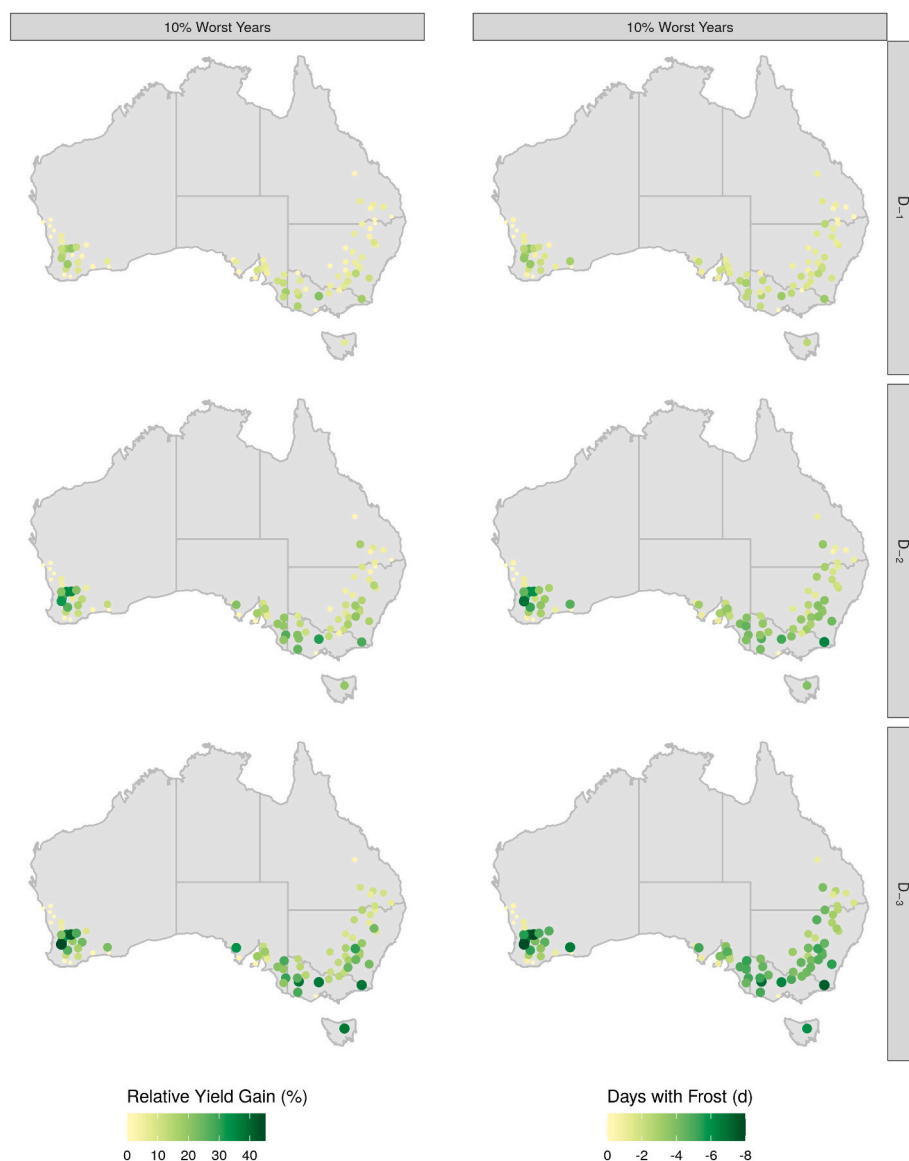


Fig. 9. Relative yield gain (%) (left column) and change in the number of frost events (days) (right column) (negative numbers mean fewer events) in the 10% worst years for yield loss, when the sensitivity to frost starts at 0 °C (D₋₁), -1 °C (D₋₂) and -2 °C (D₋₃) with respect to the default function (D = 1 °C).

Chemical approaches targeting biological ice nucleators (e.g. *Pseudomonas syringae*) have shown inconsistent efficacy in the field, and commercial products claiming to enhance freezing tolerance lack robust validation (Román-Figueroa et al., 2021). Overall, these findings reinforce that reducing frost losses will depend on resolving frost type (Kirchhof et al., 2025) and canopy microclimate, while incorporating reductions in crop sensitivity via agronomic and genetic strategies to better align crop responses with the environments that drive damage.

5. Conclusions

Spring frost continues to impose a persistent constraint on wheat yield stability under best management. Climate variability is extending and intensifying the frost risk window, reducing the effectiveness of adaptation strategies that rely primarily on cultivar choice and sowing date. Even when crops flowered within the optimal flowering period, both yield potential and water-limited yield declined over time, and frost imposed larger yield penalties than heat in severe seasons. Further

progress in adaptation and modelling remains limited by incomplete characterisation of frost types and damage pathways, insufficient representation of frost processes in crop models, and the reduced reliability of phenological escape as a stand-alone risk management strategy.

Simulation scenarios further indicate that modest reductions in crop frost sensitivity ($\approx 1\text{--}2$ °C), within the bounds of the empirical functions tested, can substantially reduce yield losses in high-risk seasons, while inducing only small shifts towards earlier optimal flowering. This suggests that yield benefits arise primarily from reduced crop sensitivity during critical reproductive stages, with additional potential benefits from improved alignment between grain number formation, seasonal water availability, and atmospheric demand, while avoiding the trade-offs typically associated with strategies that delay flowering to escape frost. More broadly, these results indicate that targeting reduced frost sensitivity provides a complementary adaptation pathway to improve the resilience of wheat systems without increasing exposure to terminal drought or heat under increasingly variable climatic conditions.

CRedit authorship contribution statement

M. Fernanda Dreccer: Writing – original draft, Supervision, Project administration, Methodology, Funding acquisition, Formal analysis, Conceptualization. **Bangyou Zheng:** Writing – review & editing, Visualization, Software, Methodology, Formal analysis, Data curation, Conceptualization. **Pengcheng Hu:** Writing – review & editing, Methodology. **Loretta Clancy:** Visualization, Software, Methodology, Data curation. **William Short:** Writing – review & editing, Conceptualization. **Karen Tanino:** Writing – review & editing, Conceptualization.

Declaration of competing interest

The authors declare no conflicts of interest.

Acknowledgements

We gratefully acknowledge Commonwealth Scientific and Industrial Research Organisation SIP228 - OD-206883 – 2017-2021 and Grains Research and Development Corporation CSP2310-008RTX. Acknowledgment is made to the APSIM Initiative which takes responsibility for quality assurance and a structured innovation programme for APSIM's modelling software, which is provided free for research and development use (see www.apsim.info for details).

Appendix A. Supplementary data

Supplementary data to this article can be found online at <https://doi.org/10.1016/j.agry.2026.104837>.

Data availability

Data will be made available on request.

References

- Adhikari, U., Nejadhashemi, A., Woznicki, S., 2015. Climate change and eastern Africa: a review of impact on major crops. *Food Energy Secur.* 4, 110–132. <https://doi.org/10.1002/fes3.61>.
- Alduchov, O.A., Eskridge, R.E., 1996. Improved Magnus form approximation of saturation vapor pressure. *J. Appl. Meteorol. Climatol.* 35, 601–609. [https://doi.org/10.1175/1520-0450\(1996\)035%253C0601:IMFAOS%253E2.0.CO;2](https://doi.org/10.1175/1520-0450(1996)035%253C0601:IMFAOS%253E2.0.CO;2).
- Asseng, S., Ewert, F., Martre, P., Rötter, R.P., Lobell, D.B., Cammarano, D., Kimball, B.A., Ottman, M.J., Wall, G.W., White, J.W., Reynolds, M.P., Alderman, P.D., Prasad, P.V. V., Aggarwal, P.K., Anothai, J., Basso, B., Biernath, C., Challinor, A.J., De Sanctis, G., Doltra, J., Fereres, E., Garcia-Vila, M., Gayler, S., Hoogenboom, G., Hunt, L.A., Izaurralde, R.C., Jabloun, M., Jones, C.D., Kersebaum, K.C., Koehler, A.-K., Müller, C., Naresh Kumar, S., Nendel, C., O'Leary, G., Olesen, J.E., Palosuo, T., Priesack, E., Eysli Rezaei, E., Ruane, A.C., Semenov, M.A., Shcherbak, I., Stöckle, C., Stratonovitch, P., Streck, T., Supit, I., Tao, F., Thorburn, P.J., Waha, K., Wang, E., Wallach, D., Wolf, J., Zhao, Z., Zhu, Y., 2015. Rising temperatures reduce global wheat production. *Nat. Clim. Chang.* 5, 143–147. <https://doi.org/10.1038/nclimate2470>.
- Barlow, K., Christy, B., O'Leary, G., Riffkin, P., Nuttall, J., 2015. Simulating the impact of extreme heat and frost events on wheat crop production: a review. *Field Crop Res.* 171, 109–119. <https://doi.org/10.1016/j.fcr.2014.11.010>.
- Boer, R., Campbell, L., Fletcher, D., 1993. Characteristics of frost in a major wheat-growing region of Australia. *Aust. J. Agric. Res.* 44, 1731–1743. <https://doi.org/10.1071/AR9931731>.
- Celestina, C., Hunt, J., Kuchel, H., Harris, F., Porker, K., Biddulph, B., Bloomfield, M., McCallum, M., Graham, R., Matthews, P., Aisthorpe, D., Al-Yaseri, G., Hyles, J., Treviskis, B., Wang, E., Zhao, Z., Zheng, B., Huth, N., Brown, H., 2023. A cultivar phenology classification scheme for wheat and barley. *Eur. J. Agron.* 143, 126732. <https://doi.org/10.1016/j.eja.2022.126732>.
- Challinor, A.J., Watson, J., Lobell, D.B., Howden, S.M., Smith, D.R., Chhetri, N., 2014. A meta-analysis of crop yield under climate change and adaptation. *Nat. Clim. Chang.* 4, 287–291. <https://doi.org/10.1038/nclimate2153>.
- Chenu, K., Dehifard, R., Chapman, S.C., 2013. Large-scale characterization of drought pattern: a continent-wide modelling approach applied to the Australian wheatbelt – spatial and temporal trends. *New Phytol.* 198, 801–820. <https://doi.org/10.1111/nph.12192>.
- Cheong, B.E., Ho, W.W.H., Biddulph, B., Wallace, X., Rathjen, T., Rupasinghe, T.W.T., Roessner, U., Dolferus, R., 2019. Phenotyping reproductive stage chilling and frost tolerance in wheat using targeted metabolome and lipidome profiling. *Metabolomics* 15, 144. <https://doi.org/10.1007/s11306-019-1606-2>.
- Crimp, S., Zheng, B., Khimashia, N., Gobbett, D., Chapman, S., Howden, M., Nicholls, N., 2016. Recent changes in southern Australian frost occurrence: implications for wheat production risk. *Crop Pasture Sci.* 67, 801–811. <https://doi.org/10.1071/CP16056>.
- Dalglish, N.P., Cocks, Brett, Horan, H., 2012. APSOil-providing soils information to consultants, farmers and researchers. In: Yunusa, I. (Ed.), 16th Australian Agronomy Conference. Capturing Opportunities and Overcoming Obstacles in Australian Agronomy. Presented at the 16th Australian Agronomy Conference. Australian Society of Agronomy, Armidale, Australia.
- Dolferus, R., Ji, X., Richards, R.A., 2011. Abiotic stress and control of grain number in cereals. *Plant Sci.* 181, 331–341. <https://doi.org/10.1016/j.plantsci.2011.05.015>.
- Dreccer, M., Fainges, J., Whish, J., Ogbonnaya, F., Sadras, V., 2018. Comparison of sensitive stages of wheat, barley, canola, chickpea and field pea to temperature and water stress across Australia. *Agric. For. Meteorol.* 248, 275–294. <https://doi.org/10.1016/j.agrformet.2017.10.006>.
- Dreccer, M., Wockner, K., Palta, J., McIntyre, C., Borgognone, M., Bourgault, M., Reynolds, M., Miralles, D., 2014. More fertile florets and grains per spike can be achieved at higher temperature in wheat lines with high spike biomass and sugar content at booting. *Funct. Plant Biol.* 41, 482–495. <https://doi.org/10.1071/FP13232>.
- Fischer, R.A., 1985. Number of kernels in wheat crops and the influence of solar radiation and temperature. *J. Agric. Sci.* 105, 447–461. <https://doi.org/10.1017/S0021859600056495>.
- Fletcher, A.L., Kirkegaard, J.A., Peoples, M.B., Robertson, M.J., Whish, J., Swan, A.D., 2016. Prospects to utilise intercrops and crop variety mixtures in mechanised, rain-fed, temperate cropping systems. *Crop Pasture Sci.* 67, 1252. <https://doi.org/10.1071/CP16211>.
- Floh, B.M., Hunt, J.R., Kirkegaard, J.A., Evans, J.R., 2017. Water and temperature stress define the optimal flowering period for wheat in South-Eastern Australia. *Field Crop Res.* 209, 108–119. <https://doi.org/10.1016/j.fcr.2017.04.012>.
- Flower, K.C., Ward, P.R., Passaris, N., Cordingley, N., 2022. Uneven crop residue distribution influences soil chemical composition and crop yield under long-term no-tillage. *Soil Tillage Res.* 223, 105498. <https://doi.org/10.1016/j.still.2022.105498>.
- Frederiks, T., Christopher, J., Harvey, G., Sutherland, M., Borrell, A., 2012. Current and emerging screening methods to identify post-head-emergence frost adaptation in wheat and barley. *J. Exp. Bot.* 63, 5405–5416. <https://doi.org/10.1093/jxb/ers215>.
- Fuller, M.P., Fuller, A.M., Kaniouras, S., Christophers, J., Fredericks, T., 2007. The freezing characteristics of wheat at ear emergence. *Eur. J. Agron.* 26, 435–441. <https://doi.org/10.1016/j.eja.2007.01.001>.
- Gama, A.B., Perondi, D., Dewdney, M.M., Fraisse, C.W., Small, I.M., Peres, N.A., 2022. Evaluation of a multi-model approach to estimate leaf wetness duration: an essential input for disease alert systems. *Theor. Appl. Climatol.* 149, 83–99. <https://doi.org/10.1007/s00704-022-04036-1>.
- García, G., Dreccer, M., Miralles, D., Serrago, R., 2015. High night temperatures during grain number determination reduce wheat and barley grain yield: a field study. *Glob. Chang. Biol.* 21, 4153–4164. <https://doi.org/10.1111/gcb.13009>.
- Gerber, J.S., Ray, D.K., Makowski, D., Butler, E.E., Mueller, N.D., West, P.C., Johnson, J.A., Polasky, S., Samberg, L.H., Siebert, S., Sloat, L., 2024. Global spatially explicit yield gap time trends reveal regions at risk of future crop yield stagnation. *Nat. Food* 5, 125–135. <https://doi.org/10.1038/s43016-023-00913-8>.
- Gobbett, D.L., Nidumolu, U., Jin, H., Hayman, P., Gallant, J., 2021. Minimum temperature mapping augments Australian grain farmers' knowledge of frost. *Agric. For. Meteorol.* 304–305, 108422. <https://doi.org/10.1016/j.agrformet.2021.108422>.
- Guo, W., Dai, H., Qian, J., Tan, J., Xu, Z., Guo, Y., 2024. An assessment of the relationship between spring frost indicators and global crop yield losses. *Sci. Total Environ.* 954, 176560.
- Gusta, L.V., Wisniewski, M., 2013. Understanding plant cold hardiness: an opinion. *Physiol. Plant.* 147, 4–14. <https://doi.org/10.1111/j.1399-3054.2012.01611.x>.
- Hochman, Z., Gobbett, D.L., Horan, H., 2017. Climate trends account for stalled wheat yields in Australia since 1990. *Glob. Chang. Biol.* 23, 2071–2081. <https://doi.org/10.1111/gcb.13604>.
- Holzworth, D., Huth, N.I., Fainges, J., Brown, H., Zurcher, E., Cichota, R., Verrall, S., Herrmann, N.I., Zheng, B., Snow, V., 2018. APSIM next generation: overcoming challenges in modernising a farming systems model. *Environ. Model. Softw.* 103, 43–51. <https://doi.org/10.1016/j.envsoft.2018.02.002>.
- Hu, P., Chapman, S.C., Dreisigacker, S., Sukumaran, S., Reynolds, M., Zheng, B., 2021. Using a gene-based phenology model to identify optimal flowering periods of spring wheat in irrigated mega-environments. *J. Exp. Bot.* 72, 7203–7218. <https://doi.org/10.1093/jxb/erab326>.
- Hunt, J.R., Lilley, J.M., Treviskis, B., Flohr, B.M., Peake, A., Fletcher, A., Zwart, A.B., Gobbett, D., Kirkegaard, J.A., 2019. Early sowing systems can boost Australian wheat yields despite recent climate change. *Nat. Clim. Chang.* 9, 244–247. <https://doi.org/10.1038/s41558-019-0417-9>.
- Jagdish, S.V.K., 2020. Heat stress during flowering in cereals – effects and adaptation strategies. *New Phytol.* 226, 1567–1572. <https://doi.org/10.1111/nph.16429>.
- Jeffrey, S.J., Carter, J.O., Moodie, K.B., Beswick, A.R., 2001. Using spatial interpolation to construct a comprehensive archive of Australian climate data. *Environ. Model. Softw.* 16, 309–330. [https://doi.org/10.1016/S1364-8152\(01\)00008-1](https://doi.org/10.1016/S1364-8152(01)00008-1).
- Kim, Y.-U., Asseng, S., Webber, H., 2025. Spring frost risk assessment on winter wheat in South Korea. *Agric. For. Meteorol.* 366, 110484. <https://doi.org/10.1016/j.agrformet.2025.110484>.
- Kirchof, E., Campos-Arguedas, F., Arias, N.S., Kovaleski, A.P., 2025. Thresholds for spring freeze: measuring risk to improve predictions in a warming world. *New Phytol.* <https://doi.org/10.1111/nph.70453>.

- Lawes, R.A., Roche, R., Darbyshire, R.O., Singaram Natarajan, A., Herrmann, C.M., 2025. Contrasting trends in wheat production exist across Australia in response to climate. *Eur. J. Agron.* 171, 127785. <https://doi.org/10.1016/j.eja.2025.127785>.
- Lesk, C., Rowhani, P., Ramankutty, N., 2016. Influence of extreme weather disasters on global crop production. *Nature* 529, 84. <https://doi.org/10.1038/nature16467>.
- Li, X., Cai, J., Liu, F., Dai, T., Cao, W., Jiang, D., 2015. Spring freeze effect on wheat yield is modulated by winter temperature fluctuations: evidence from meta-analysis and simulating experiment. *J. Agron. Crop Sci.* 201, 288–300.
- Lilley, J.M., Flohr, B.M., Whish, J.P.M., Farre, I., Kirkegaard, J.A., 2019. Defining optimal sowing and flowering periods for canola in Australia. *Field Crop Res.* 235, 118–128. <https://doi.org/10.1016/j.fcr.2019.03.002>.
- Livingston, D.P., Tuong, T.D., Isleib, T.G., Murphy, J.P., 2016. Differences between wheat genotypes in damage from freezing temperatures during reproductive growth. *Eur. J. Agron.* 74, 164–172. <https://doi.org/10.1016/j.eja.2015.12.002>.
- Livingston, D.P., Tuong, T.D., Murphy, J.P., Gusta, L.V., Willick, I., Wisniewski, M.E., 2018. High-definition infrared thermography of ice nucleation and propagation in wheat under natural frost conditions and controlled freezing. *Planta* 247, 791–806. <https://doi.org/10.1007/s00425-017-2823-4>.
- Livingston, D.P., Bertrand, A., Wisniewski, M., Tisdale, R., Tuong, T., Gusta, L.V., Artlip, T., 2021. Factors contributing to ice nucleation and sequential freezing of leaves in wheat. *Planta* 253, 124. <https://doi.org/10.1007/s00425-021-03637-w>.
- Lobell, D.B., Field, C.B., 2007. Global scale climate–crop yield relationships and the impacts of recent warming. *Environ. Res. Lett.* 2, 014002. <https://doi.org/10.1088/1748-9326/2/1/014002>.
- Marcellos, H., Single, W., 1975. Temperatures in wheat during radiation frost. *Aust. J. Exp. Agric. Anim. Husb.* 15, 818–822. <https://doi.org/10.1071/EA9750818>.
- Martínez-Subirá, M., Romero, M.-P., Moralejo, M., Macià, A., Puig, E., Savin, R., Romagosa, I., 2021. Post-anthesis thermal stress induces differential accumulation of bioactive compounds in field-grown barley. *J. Sci. Food Agric.* 101, 6496–6504. <https://doi.org/10.1002/jsfa.11321>.
- Perry, E.M., Nuttall, J.G., Wallace, A.J., Fitzgerald, G.J., 2017. In-field methods for rapid detection of frost damage in Australian dryland wheat during the reproductive and grain-filling phase. *Crop Pasture Sci.* 68, 516–526.
- Porker, K., Kupke, B., Hunt, J., Ware, A., Thomas, D., Cooper, B., 2022. Apical Pruning to Delay Flowering Time and Increase Yield in Early Sown Spring Wheat.
- Rahman, T., Shao, M., Pahari, S., Venglat, P., Soolanayakanahally, R., Qiu, X., Rahman, A., Tanino, K., 2021. Dissecting the roles of cuticular wax in plant resistance to shoot dehydration and low-temperature stress in Arabidopsis. *Int. J. Mol. Sci.* 22, 1554.
- Rapacz, M., Macko-Podgórn, A., Jurczyk, B., Kuchar, L., 2022. Modeling wheat and triticale winter hardiness under current and predicted winter scenarios for Central Europe: a focus on deacclimation. *Agric. For. Meteorol.* 313, 108739. <https://doi.org/10.1016/j.agrformet.2021.108739>.
- Rebbeck, M., Lynch, C., Hayman, P.T., Sadras, V.O., 2007. Delving of sandy surfaced soils reduces frost damage in wheat crops. *Aust. J. Agric. Res.* 58, 105. <https://doi.org/10.1071/AR06097>.
- Rebetzke, G.J., Richards, R.A., Fettel, N.A., Long, M., Condon, A.G., Forrester, R.I., Botwright, T.L., 2007. Genotypic increases in coleoptile length improves stand establishment, vigour and grain yield of deep-sown wheat. *Field Crops Res.* 100, 10–23. <https://doi.org/10.1016/j.fcr.2006.05.001>.
- Richetti, J., Sadras, V.O., He, D., Leske, B., Hu, P., Beletse, Y., Cossani, C.M., Nguyen, H., Zheng, B., Deery, D.M., Dreccer, M.F., Whish, J., Lilley, J., 2025. Challenges in modelling the impact of frost and heat stress on the yield of cool-season annual grain crops. *Front. Plant Sci.* 16.
- Rodriguez, D., Serafin, L., de Voil, P., Mumford, M., Zhao, D., Aisthorpe, D., Auer, J., Broad, I., Eyre, J., Hellyer, M., 2024. Agronomic adaptations to heat stress: sowing summer crops earlier. *Field Crop Res.* 318, 109592. <https://doi.org/10.1016/j.fcr.2024.109592>.
- Román-Figueroa, C., Bravo, L., Paneque, M., Navia, R., Cea, M., 2021. Chemical products for crop protection against freezing stress: a review. *J. Agron. Crop Sci.* 207, 391–403. <https://doi.org/10.1111/jac.12489>.
- Sadras, V., Dreccer, M., 2015. Adaptation of wheat, barley, canola, field pea and chickpea to the thermal environments of Australia. *Crop Pasture Sci.* 66, 1137–1150. <https://doi.org/10.1071/CP15129>.
- Santer, B.D., Wigley, T.M.L., Boyle, J.S., Gaffen, D.J., Hnilo, J.J., Nychka, D., Parker, D. E., Taylor, K.E., 2000. Statistical significance of trends and trend differences in layer-average atmospheric temperature time series. *J. Geophys. Res. Atmos.* 105, 7337–7356. <https://doi.org/10.1029/1999JD901105>.
- Sentelhas, P.C., Dalla Marta, A., Orlandini, S., Santos, E.A., Gillespie, T.J., Gleason, M.L., 2008. Suitability of relative humidity as an estimator of leaf wetness duration. *Agric. For. Meteorol.* 148, 392–400. <https://doi.org/10.1016/j.agrformet.2007.09.011>.
- Stefan, L., Fossati, D., Camp, K., Pellet, D., Foiada, F., Levy, L., 2024. Asynchrony is more important than genetic distance in driving yield stability in wheat variety mixtures. *Crop Sci.* 64, 455–469. <https://doi.org/10.1002/csc2.21151>.
- Single, W., Marcellos, H., 1974. Studies on frost injury to wheat. IV. Freezing of ears after emergence from the leaf sheath. *Aust. J. Agric. Res.* 25, 679–686. <https://doi.org/10.1071/AR9740679>.
- Stefan, L., Colbach, N., Fossati, D., Strebel, S., Häner, L.L., 2025. Plasticity in Ear Density Drives Complementarity Effects and Yield Benefits in Wheat Variety Mixtures. <https://doi.org/10.1101/2025.02.25.640070>.
- Stone, P., Nicolas, M., 1995. Comparison of sudden heat stress with gradual exposure to high temperature during grain filling in two wheat varieties differing in heat tolerance. I. grain growth. *Funct. Plant Biol.* 22, 935–944. <https://doi.org/10.1071/PP950935>.
- Subedi, R., Naiker, M., Chauhan, Y., Jagadish, S.V.K., Bhattarai, S.P., 2025. Wheat under warmer nights: shifting of sowing dates for managing impacts of thermal stress. *Agriculture* 15 (15), 1687. <https://doi.org/10.3390/agriculture15151687>.
- Wang, E., Brown, H., Zheng, B., Zhao, Z., Huth, N., Hunt, J.R., Hyles, J., Bloomfield, M., Celestina, C., Porker, K., Harris, F., Biddulph, B., Stefanova, K., Trevaskis, B., 2025. Molecular–physiological model integration revolutionizes cereal flowering prediction. *New Phytol.* <https://doi.org/10.1111/nph.70651>.
- Webber, H., Martre, P., Asseng, S., Kimball, B., White, J., Ottman, M., Wall, G.W., De Sanctis, G., Doltra, J., Grant, R., Kassie, B., Maiorano, A., Olesen, J.E., Ripoche, D., Rezaei, E.E., Semenov, M.A., Stratonovitch, P., Ewert, F., 2017. Canopy temperature for simulation of heat stress in irrigated wheat in a semi-arid environment: a multi-model comparison. *Model. Crops Genotype Phenotype Chang. Clim.* 202, 21–35. <https://doi.org/10.1016/j.fcr.2015.10.009>.
- Wichink Kruit, R.J., van Pul, W.A.J., Jacobs, A.F.G., Heusinkveld, B.G., 2004. Comparison between four methods to estimate leaf wetness duration caused by dew on grassland. In: 26th Conference on Agricultural and Forest Meteorology (26AG), Boston. Presented at the 26th Conference on Agricultural and Forest Meteorology (26AG). American Meteorological Society, Boston, p. 10.1.
- Wisniewski, M.E., Gusta, L.V., Fuller, M.P., Karlson, D., 2009. Ice nucleation, propagation and deep supercooling: The lost tribes of freezing studies. In: Gusta, L. V., Wisniewski, M.E., Tanino, K.K. (Eds.), *Plant Cold Hardiness: From the Laboratory to the Field*. CAB, UK, pp. 1–11. <https://doi.org/10.1079/9781845935139.0001>.
- Xiao, L., Asseng, S., Wang, X., Xia, J., Zhang, P., Liu, L., Tang, L., Cao, W., Zhu, Y., Liu, B., 2022. Simulating the effects of low-temperature stress on wheat biomass growth and yield. *Agric. For. Meteorol.* 326, 109191. <https://doi.org/10.1016/j.agrformet.2022.109191>.
- Zhao, Y., Xiao, L., Tang, Y., Yao, X., Cheng, T., Zhu, Y., Cao, W., Tian, Y., 2024. Spatio-temporal change of winter wheat yield and its quantitative responses to compound frost-dry events - an example of the Huang-Huai-Hai plain of China from 2001 to 2020. *Sci. Total Environ.* 940. <https://doi.org/10.1016/j.scitotenv.2024.173531>.
- Zheng, B., Chenu, K., Dreccer, M., Chapman, S., 2012. Breeding for the future: what are the potential impacts of future frost and heat events on sowing and flowering time requirements for Australian bread wheat (*Triticum aestivum*) varieties? *Glob. Chang. Biol.* 18, 2899–2914. <https://doi.org/10.1111/j.1365-2486.2012.02724.x>.
- Zheng, B., Chapman, S.C., Christopher, J.T., Frederiks, T.M., Chenu, K., 2015. Frost trends and their estimated impact on yield in the Australian wheatbelt. *J. Exp. Bot.* 66, 3611–3623. <https://doi.org/10.1093/jxb/erv163>.
- Zheng, B., Chenu, K., Chapman, S.C., 2016. Velocity of temperature and flowering time in wheat – assisting breeders to keep pace with climate change. *Glob. Chang. Biol.* 22, 921–933. <https://doi.org/10.1111/gcb.13118>.
- Zohner, C.M., Mo, L., Renner, S.S., Svenning, J.-C., Vitasse, Y., Benito, B.M., Ordóñez, A., Baumgarten, F., Bastin, J.-F., Sebald, V., Reich, P.B., Liang, J., Nabuurs, G.-J., de Miguel, S., Alberti, G., Anton Fernandez, C., Balazy, R., Brandli, U.B., Chen, H.Y.H., Chisholm, C., Cienciala, E., Dayanandan, S., Fayle, T.M., Frizzera, L., Gianelle, D., Jagodzinski, A.M., Jaroszewicz, B., Jucker, T., Kepfer Rojas, S., Khan, M.L., Kim, H. S., Korjus, H., Johannsen, V.K., Laarmann, D., Lang, M., Zawila-Niedzwiecki, T., Niklaus, P.A., Paquette, A., Pretzsch, H., Saikia, P., Schall, P., Šeběn, V., Svoboda, M., Tikhonova, E., Viana, H., Zhang, C., Zhao, X., Crowther, T.W., 2020. Late-spring frost risk between 1959 and 2017 decreased in North America but increased in Europe and Asia. *Proc. Natl. Acad. Sci.* 117, 12192–12200. <https://doi.org/10.1073/pnas.1920816117>.